Korean J. Chem. Eng., 34(7), 1896-1904 (2017)
DOI: 10.1007/s11814-017-0059-4

pISSN: 0256-1115
eISSN: 1975-7220

Effect of sinusoidal Taylor vortex flow on cooling crystallization of L-lysine

Anh-Tuan Nguyen and Woo-Sik Kim†

Department of Chemical Engineering, Functional Crystallization Center, Kyung Hee University, Seocheon-dong, Giheung-gu, Yongin-si 17104, Korea
(*Received 25 November 2016 • accepted 3 March 2017*)

Abstract−An elliptical Couette-Taylor (ECT) crystallizer with a unique sinusoidal Taylor vortex flow was developed to promote the recovery and size distribution of L-lysine crystals in cooling crystallization. When using the ECT crystallizer, the recovery was enhanced to a maximum of 100% with a mean residence time of only 15 min. When comparing the crystallization efficiency, the recovery and size distribution of the L-lysine crystals in the ECT crystallizer were over 33% and 50% higher, respectively, than those in the conventional MSMPR crystallizer and slightly higher than those in the circular Couette-Taylor (CT) crystallizer. This improved crystallization in the ECT crystallizer was explained in terms of the sinusoidal profile of the Taylor vortex intensity. Plus, since the nucleation and growth processes determine the recovery and crystal size distribution, the mean residence time, inner cylinder rotation speed, and feed concentration were all varied to investigate their influence on the crystallization efficiency.

Keywords: Taylor Vortex Flow, Cooling Crystallization, Nucleation, Growth, Mass Transfer, Couette-Taylor Crystallizer

INTRODUCTION

Fluid hydrodynamics are a key factor in crystallization, influencing important characteristics of crystal product such as the crystal recovery (yield), crystal shape, crystal size distribution, crystal structure and purity [1].

A Taylor vortex flow is known as a unique periodical and circular fluid motion that is induced in the gap between two co-axial cylinders when one is rotating and provides homogeneous radial mixing with a small axial dispersion. Taylor vortex flows are already widely applied in such areas as crystallization [2], polymerization [3], membrane separation [4], photocatalytic reactions [5], filtration [6], and biological systems [7]. For example, Kim et al. [2] reported that the recovery of GMP crystal products is significantly enhanced under a Taylor vortex flow in a Couette-Taylor (CT) crystallizer when compared with the recovery in a conventional MSMPR crystallizer. In this case, the recovery from the CT crystallizer was 100% with a mean residence time of only 7 minutes in the CT crystallizer, whereas it required a mean residence time of at least 6 hours in the conventional MSMPR crystallizer. This remarkable result is explained by the high mass transfer facilitated by the Taylor vortex flow, thereby promoting the nucleation and growth processes of the hydrate GMP crystals and enhancing the crystal product recovery. Plus, a Taylor vortex flow was reported to promote the mass transfer of the gas-liquid (CO_2-$Ca(OH)_2$) reaction in $CaCO_3$ crystallization, resulting in a more uniform crystal size and shape of the $CaCO_3$ product in the CT crystallizer when compared to the product in the conventional MSMPR crystallizer [8,9].

To amplify the periodic effect of a Taylor vortex flow, the configuration of the cylinders was also modified. For example, Dluska et al. developed an eccentric Taylor reactor, in which the circular inner cylinder is eccentrically aligned with the outer cylinder to induce an asymmetric fluid motion in the gap, called an eccentric Taylor vortex. As a result, the gas-liquid mass transfer rate in an eccentric Taylor reactor is significantly improved when compared with the rates in a conventional stirred tank reactor and concentric Taylor reactor. This enhanced mass transfer rate is attributed to the asymmetric variation of the pressure and velocity of the eccentric fluid motion. Czarnetzki et al. [10] also modified the geometry of the inner cylinder by installing rib rings on the surface of the inner cylinder, resulting in increased turbulent micro-mixing as the Taylor vortex between the rib rings is immobilized and stabilized. Meanwhile, Noui-Mehidi et al. [11] demonstrated a 10% improvement in the mass transfer of viscous fluid in a co-axial conical Taylor reactor when compared to that in a normal Taylor reactor due to the swirling motion of the fluid generated by the conical geometry.

Previously, the unique Taylor vortex flow in a CT crystallizer was shown to improve the recovery and size distribution of L-lysine crystal products when compared with the results from a conventional MSMPR crystallizer [12]. Accordingly, to further enhance the recovery and size distribution, we applied a sinusoidal Taylor vortex flow in an elliptical Couette-Taylor crystallizer (ECT). The cross-section of the inner cylinder was designed as elliptical and co-axially aligned with the circular outer cylinder so the gap dimension between the two cylinders varied along with the angular direction. The sinusoidal fluctuation of the fluid motion, called a sinusoidal Taylor vortex, was induced by rotating the inner cylinder in the ECT crystallizer. The effect of the sinusoidal Taylor vortex flow on the recovery, crystal size, and size distribution was then investigated. The efficiency of the ECT crystallizer was also com-

†To whom correspondence should be addressed.
E-mail: wskim@khu.ac.kr
‡This article is dedicated to Prof. Ki-Pung Yoo on the occasion of his retirement from Sogang University.

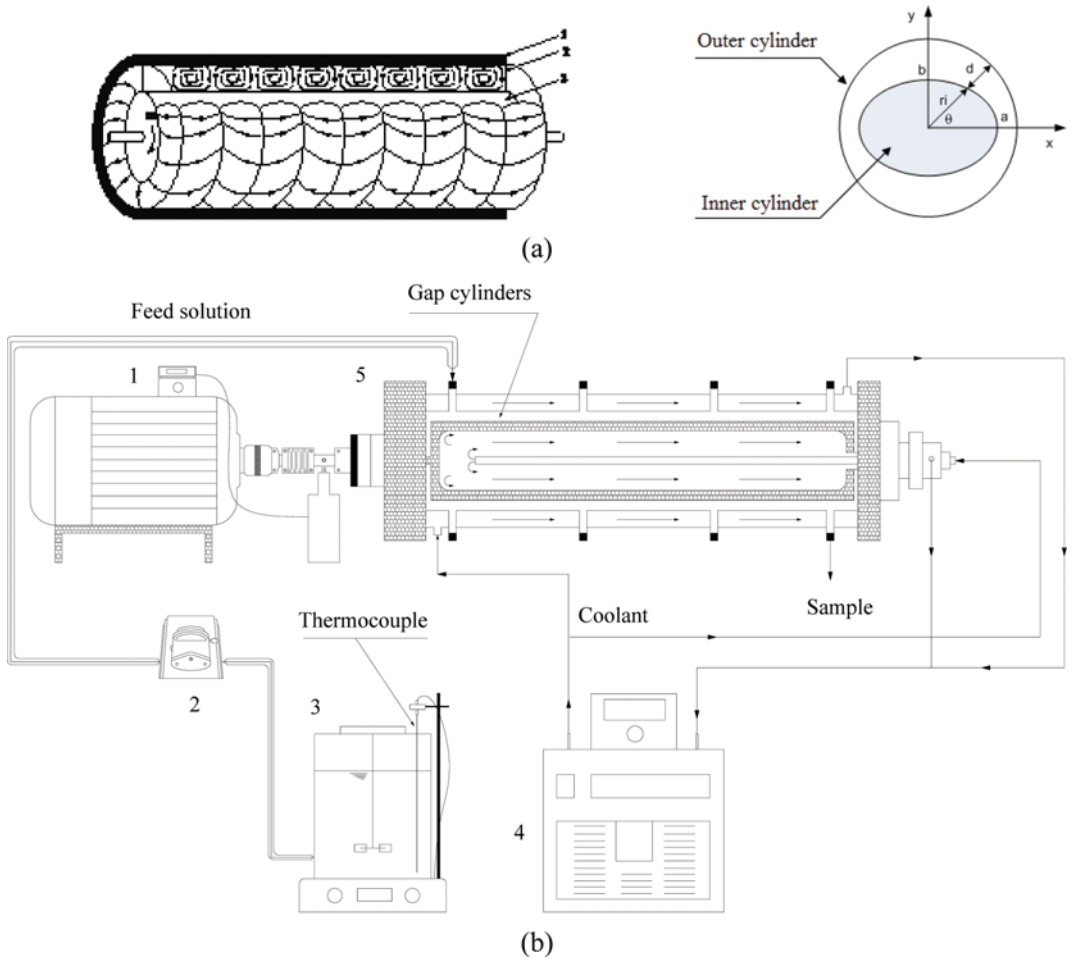

Fig. 1. (a) Schematic drawings of sinusoidal Taylor vortex flows (1. Stationary outer cylinder; 2. Taylor vortices; 3. Rotating inner cylinder) and (b) experimental system for elliptical CT crystallizer (1. DC motor; 2. Pump; 3. L-Lysine feed solution; 4. Chiller; 5. Elliptical Couette-Taylor crystallizer).

pared with that of a conventional MSMPR and conventional circular Couette-Taylor crystallizer. The mean residence time, inner cylinder rotation speed, and feed concentration were all considered as the key operating factors of the crystallization in the crystallizers.

2. Theoretical Background

The intensity of a turbulent fluid motion is often quantified in terms of the viscous energy dissipation per unit mass of solution. Thus, the viscous energy dissipation (ε) of a Taylor vortex flow has been suggested as [13,14]

$$\varepsilon=\left(\frac{0.8\pi L_C \upsilon^{0.53}\omega_i^{2.47}}{V_R}\right) r_i^{3.12} d^{-0.18} \quad (1)$$

where L_C and V_R are the length and volume of the crystallizer, respectively, r_i is the radius of the inner cylinder, and ω_i is the angular velocity of the inner cylinder. Also, is the kinematic viscosity of the solution and d is the gap between the two cylinders. According to Eq. (1), the intensity of a Taylor vortex depends directly on the geometry factors of the crystallizer, r_i and d. In a circular CT crystallizer, the geometry factors remain constant along the circumference of the cylinders. However, in an ECT crystallizer, the geometry factors vary periodically with the angular position of the inner cylinder. Thus, Eq. (1) was used to estimate the sinusoidal fluctuation of the viscous energy dissipation in the ECT crystallizer shown in Fig. 1.

Similarly, the mass transfer in a sinusoidal Taylor vortex flow can be estimated by using the Sherwood number correlated in a circular Taylor vortex flow, as follows [15]:

$$Sh=2+0.4\left(\frac{d_p^{0.53}\omega_i^{0.53}}{\upsilon^{0.2}D_f^{0.33}}\right) r_i^{0.265} d^{0.265} \quad (2)$$

where d_p indicates the diameter of the solid particles and D_f is the diffusion coefficient. In this study, the viscous energy dissipation and mass transfer in the mixing tank crystallizers were estimated as reported in previous studies [16,17].

EXPERIMENTAL

The continuous cooling crystallization of L-lysine was in an elliptical Couette-Taylor (ECT) crystallizer made of stainless steel, as shown in Fig. 1. The geometric dimensions of the ECT and CT crystallizers are summarized in Table 1. The design of the MSMPR

Table 1. Dimensions of Couette-Taylor crystallizer

Length of cylinders: L_C	30×10^{-2} m	
Radius of outer cylinder: r_o	2.8×10^{-2} m	
Circular CT crystallizer (CT)	Radius of circle inner cylinder: r_i	2.4×10^{-2} m
	Gap between two circle cylinders: d	0.4×10^{-2} m
Elliptical CT crystallizer (ECT)	Radius of elliptical inner cylinder	
	Major radius: a	2.5×10^{-2} m
	Minor radius: b	2.3×10^{-2} m
	Gap between a and r_o: d_1	0.3×10^{-2} m
	Gap between b and r_o: d_2	0.5×10^{-2} m

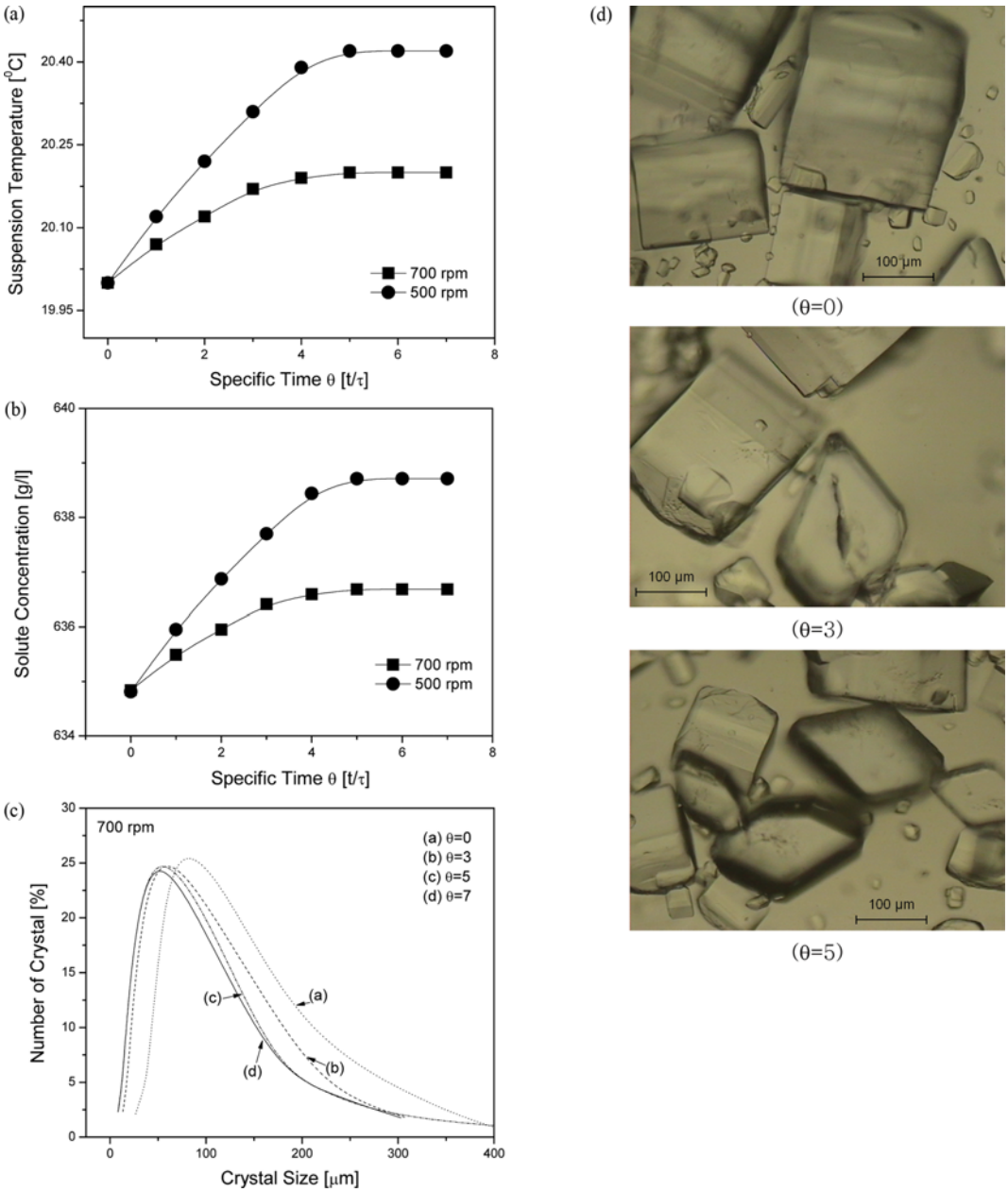

Fig. 2. Typical transient period from unsteady to steady state in cooling crystallization of L-Lysine when using feed solution temperature of 50 °C, cooling temperature of 20 °C, feed concentration of 900 g/l, and 5-min mean residence time: (a) suspension temperature, (b) solute concentration, (c) crystal size distribution at 700 rpm, and (d) crystal shape at 700 rpm.

crystallizer was based on a standard Rushton mixing tank [16]. For comparison, the CT and MSMPR crystallizers were designed to have the same working volume as the ECT crystallizer. The inner cylinders of the ECT and CT crystallizers were rotated using a DC motor. The rotation speed was varied from 300 to 900 rpm. Impeller agitation was also applied to the suspension in the MSMPR crystallizer, varying from 300 to 900 rpm. A chiller was used to control the temperature of the crystallizers. In the ECT and CT crystallizers, the temperature of the suspension was controlled by cooling both the inner and outer cylinders, while a cooling jacket was applied to the outer wall of the MSMPR crystallizer.

The raw L-lysine mono-hydrochloride (99% purity) supplied by CJ Co. (Korea) was used without any further purification. The L-lysine feed solution was prepared by dissolving the raw material in distilled water. The feed concentration was varied from 850-1,000 g/*l* at a fixed temperature of 50 °C. Initially, the crystallizers were filled with the lysine solution and cooled to 20 °C in the batch mode. The feed solution was then continuously fed into the crystallizer through an inlet port located at one end of the crystallizer using pumps (LongerPump, USA). The flow rate of the feed solution was varied from 3.26 ml/min to 78.4 ml/min to change the mean residence time in the crystallizer from 2.5 to 60 min.

Product samples were taken from the crystallizers and quickly filtered with a vacuum pump. The solid samples were then dried in a desiccator to analyze the crystal size, shape, and structure. The crystal size was measured by video microscope (IT System, Sometech, USA). The crystal structure of the L-lysine was confirmed by using an XRD (X-ray diffractometer, MAC Science, M18XHF-SRA, CuK_a line, Japan) and thermogravimetric analysis (TGA). The solute concentration in the solution was monitored by using a UV-Vis (JASCO, V-570, USA).

RESULTS AND DISCUSSION

1. Cooling Crystallization of L-lysine in ECT Crystallizer

The typical transition stages from an unsteady state to a steady state of cooling crystallization in the ECT crystallizer are illustrated in Fig. 2. During the transition stages, the solute concentration and suspension temperature gradually increased and achieved an invariable value after five-times the mean residence time, indicating a steady state of crystallization (Fig. 2(a)-(b)). In addition, the invariable crystal size and size distribution after five-times the mean residence time also confirmed a steady state for the product stream, as shown in Fig. 2(c). The typical shape of the crystal products is displayed in Fig. 2(d). Here, cooling crystallization of L-Lysine obviously depended on the fluid hydrodynamic, where the suspension temperature and solute concentration were both lower at 700 rpm than at 500 rpm (Fig. 2(a)-(b)).

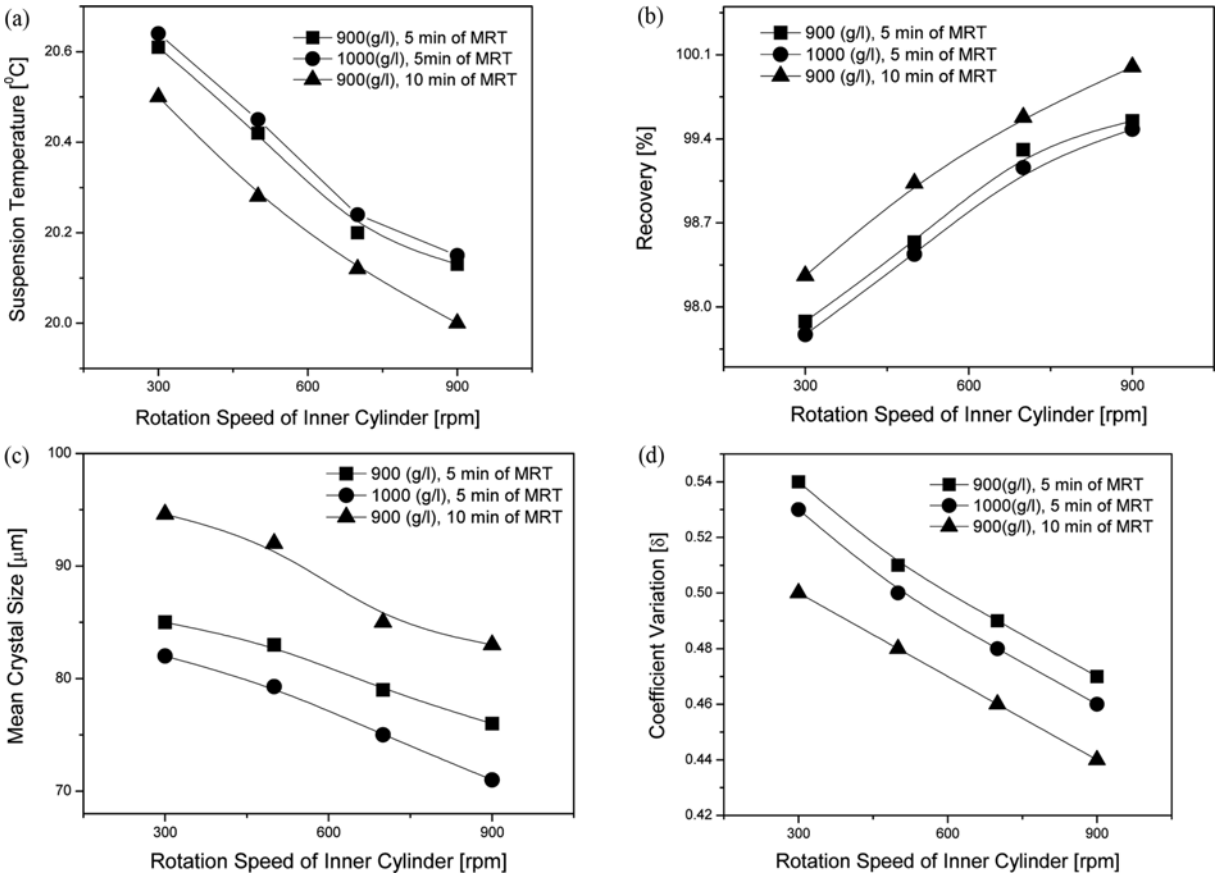

Fig. 3. Influence of rotation speed with various feed concentrations and mean residence times on recovery, suspension temperature, crystal size, and size distribution in cooling crystallization of L-Lysine when using feed solution temperature of 50 °C and cooling temperature of 20 °C.

As the recovery, crystal size, and size distribution all depend on the nucleation and growth processes, the effect of the crystallization conditions, including the rotation speed of the inner cylinder, mean residence time, and feed concentration, was investigated at a steady state. Fig. 3 shows that the suspension temperature, recovery, crystal size, and size distribution were all dependent on the rotation speed of the inner cylinder. When increasing the rotation speed from 300 rpm to 900 rpm, the suspension temperature decreased from 20.7 °C to 20 °C; meanwhile, the crystal product recovery increased from 97.7% to 100% when varying the mean residence time and feed concentration (Fig. 3(a)-(b)). Furthermore, the crystal size and size distribution became smaller and narrower, respectively, when increasing the rotation speed, as shown in Fig. 3(c)-(d).

Since the heat transfer of a Taylor vortex flow depends directly on the Taylor number (Ta) that correlates with the rotation speed of the inner cylinder, the heat transfer was promoted when increasing the rotation speed, thereby decreasing the suspension temperature (Fig. 3(a)). According to the solubility data [12], the recovery was certainly enhanced when decreasing the suspension temperature. Plus, the vortex intensity of the fluid motion in the ECT crystallizer flow was enhanced when increasing the rotation speed, promoting both the crystal nucleation and growth processes. As regards the crystal recovery, the promotion of crystal nucleation and growth contributed to enhancing the amount of crystals in the suspension (Fig. 3(b)). Notwithstanding, a high vortex intensity promoting crystal nucleation and growth had a contradictory influence on the crystal size. While the intensive vortex flow improved the mass transfer rate for crystal growth, it also created a high supersaturation at the inlet region due to rapid cooling of the feed solution [12]. Consequently, the high nucleation of crystals in the inlet region resulted in small crystals in the product suspension. In general, since crystal nucleation is more sensitive to supersaturation than crystal growth, the crystal nucleation predominantly determines the crystal size in the product suspension. Therefore, the crystal size of L-lysine was reduced when increasing the rotation speed in the ECT crystallizer (Fig. 3(c)). Moreover, the total surface area of crystals was enhanced when increasing the nucleation rate, which quickly decreased the supersaturation due to crystal growth, prevented secondary nucleation, and resulted in a

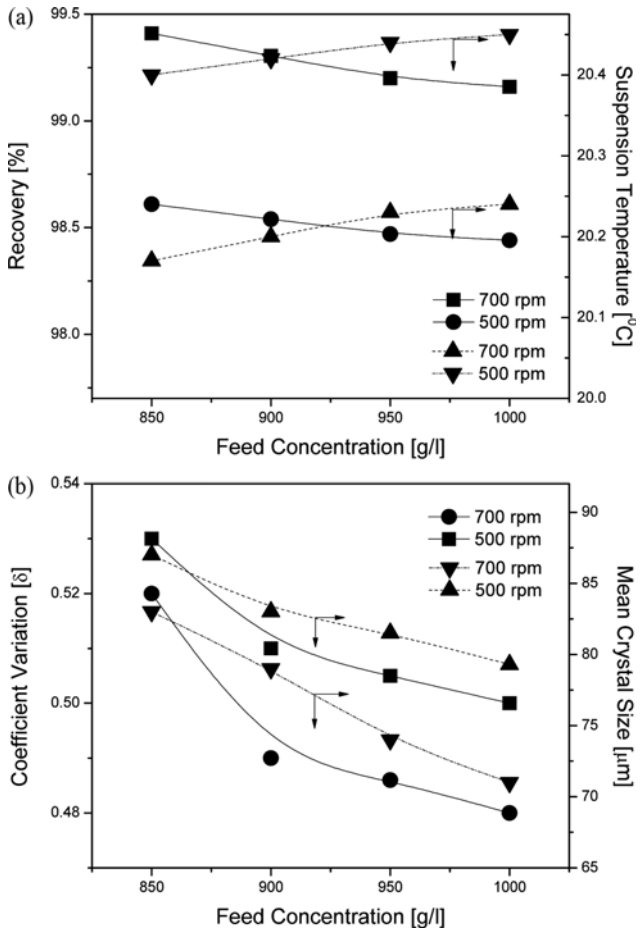

Fig. 4. Influence of feed concentration with various rotation speeds on recovery, crystal size, and size distribution in cooling crystallization of L-Lysine when using feed solution temperature of 50 °C, cooling temperature of 20 °C, and 5-min mean residence time.

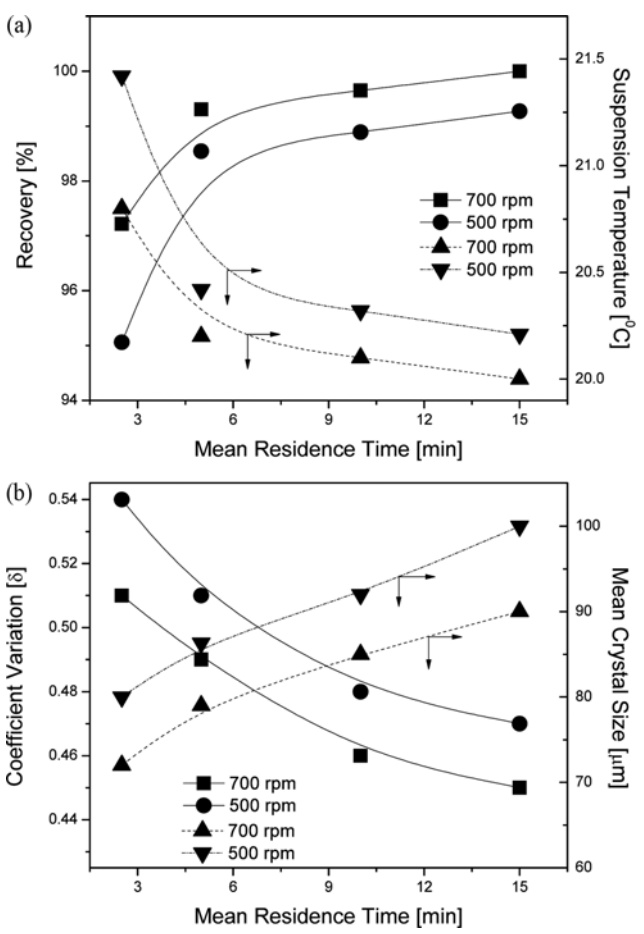

Fig. 5. Influence of mean residence time with various rotation speeds on recovery, suspension temperature, crystal size, and size distribution in cooling crystallization of L-Lysine when using feed solution temperature of 50 °C, cooling temperature of 20 °C, and feed concentration of 900 g/l.

narrower size distribution, as shown in Fig. 3(d). Since a high feed concentration consistently induced a high supersaturation, the crystal size and size distribution became smaller and narrower when increasing the feed concentration (Fig. 4). As shown in Fig. 4(a)), the recovery was slightly decreased when increasing the feed concentration. This indicated that when using a fixed rotation speed, since the consumption of solute molecules in the solution by crystal growth remained invariant, the solute concentration increased when increasing the feed concentration, resulting in a decreased recovery (Fig. 4(a)). Thus, the fluid hydrodynamic conditions were identified as important factors controlling crystal growth, which is the primary determinant for L-Lysine crystal product recovery.

As shown in Fig. 5, the recovery and crystal size distribution varied remarkably with the mean residence time. When increasing the mean residence time from 2.5 min to 15 min, the crystal recovery was significantly enhanced from 95% to 100%. In addition, the crystal size distribution became narrower, corresponding to a decrease in the coefficient variation (δ) from 0.54 to 0.45 when increasing the mean residence time. These results were due to a high heat-mass transfer and low supersaturation in the crystallizer

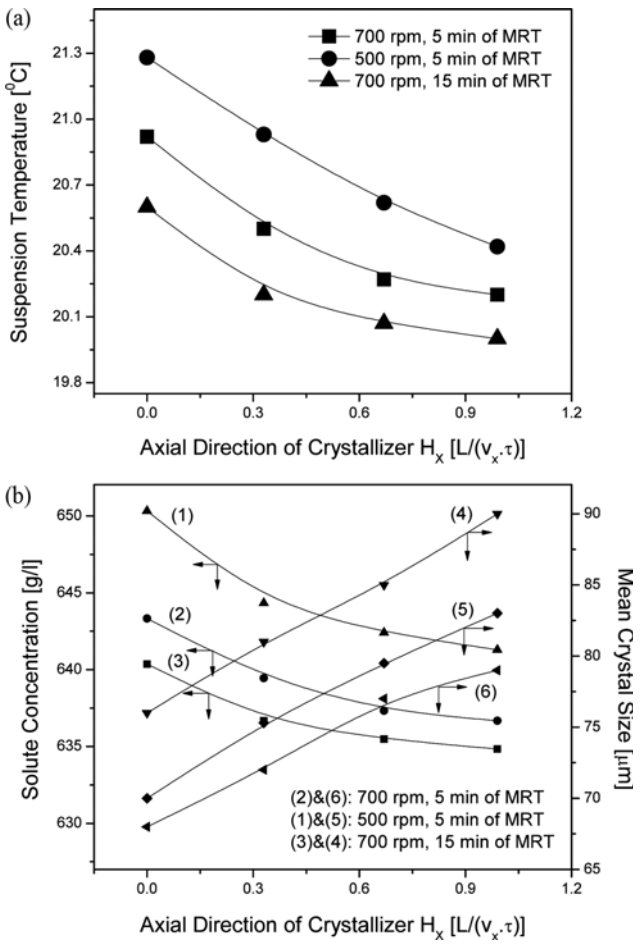

Fig. 6. Typical axial profiles for solute concentration, suspension temperature, and crystal size in cooling crystallization of L-Lysine with various rotation speeds and mean residence times when using feed solution temperature of 50 °C, cooling temperature of 20 °C, and L-Lysine feed concentration of 900 g/*l*.

when increasing the mean residence time [18]. Thus, the flow rate of the feed solution was reduced when increasing the mean residence time, which allowed an increase in the heat-mass transfer, along with an increased recovery and decrease in the suspension temperature (Fig. 5(a)). Moreover, the supersaturation decreased when increasing the mean residence time, which then reduced the nucleation rate and secondary nucleation, and resulted in an enhanced crystal size with a narrower size distribution (Fig. 5(b)). Here, it is interesting that the sinusoidal Taylor vortex flow in the ECT crystallizer was very effective in promoting the crystal product recovery, which reached 100% after a mean residence time of only 15 min.

To understand the crystallization behavior in the ECT crystallizer, the suspension temperature, solute concentration and crystal size profiles were monitored along the axial position in the crystallizer at a steady state, as shown in Fig. 6. The crystallization proceeded along the axial direction of the crystallizer. Thus, the crystal size increased gradually, based on consuming the supersaturation along the axial direction, which also resulted in a gradual decrease in the solute concentration in the crystallizer. Furthermore, the solute concentration along the axial direction of the crystallizer was much lower than that of the feed concentration (900 g/*l*), which indicated that the crystal nucleation of L-lysine mostly occurred around the inlet region of the crystallizer, while the crystal growth proceeded in the subsequent regions of the crystallizer.

2. Comparison of Crystallizers

The crystallization efficiency of the ECT crystallizer was compared with the efficiency of the MSMPR and CT crystallizers, as shown in Fig. 7. The crystallization in the ECT and CT crystallizers was more efficient than that in the MSMPR across the whole range of mean residence times. Here, the crystal recovery in the ECT was 33% higher than that in the MSMPR crystallizer with a mean residence time of 5 min, and reached 100% with a mean residence time of 15 min. In contrast, the MSMPR crystallizer required a mean residence time of 60 min of (Fig. 7(a)). Furthermore, the size distribution of L-Lysine crystals in the ECT crystallizer was significantly enhanced by more than 50% when compared to the size distribution in the conventional MSMPR crystallizer (Fig. 7(b)). Notwithstanding, the ECT produced smaller crystals than the MSMPR crystallizer (Fig. 7(c)). When comparing the ECT and CT crystallizers, the recovery and size distribution of the L-lysine crystal products in the ECT crystallizer were slightly better than those in the CT crystallizer.

Based on the above experimental results, the periodic Taylor vortex flow in the ECT and CT crystallizers was shown to be much more effective for the cooling crystallization of L-lysine than the random turbulent eddy in the MSMPR crystallizer. In addition, the sinusoidal fluid motion in the ECT crystallizer improved the crystallization efficiency slightly more than the circular azimuthal fluid motion in the CT crystallizer.

To understand the effects of the fluid dynamics on the crystallization, the viscous energy dissipations and mass transfers of the periodic Taylor vortices and turbulent eddy were estimated, as shown in Fig. 8. The sinusoidal fluid motion in the ECT crystallizer created sinusoidal profiles for the viscous energy dissipation and mass transfer along an angular direction. It was interesting

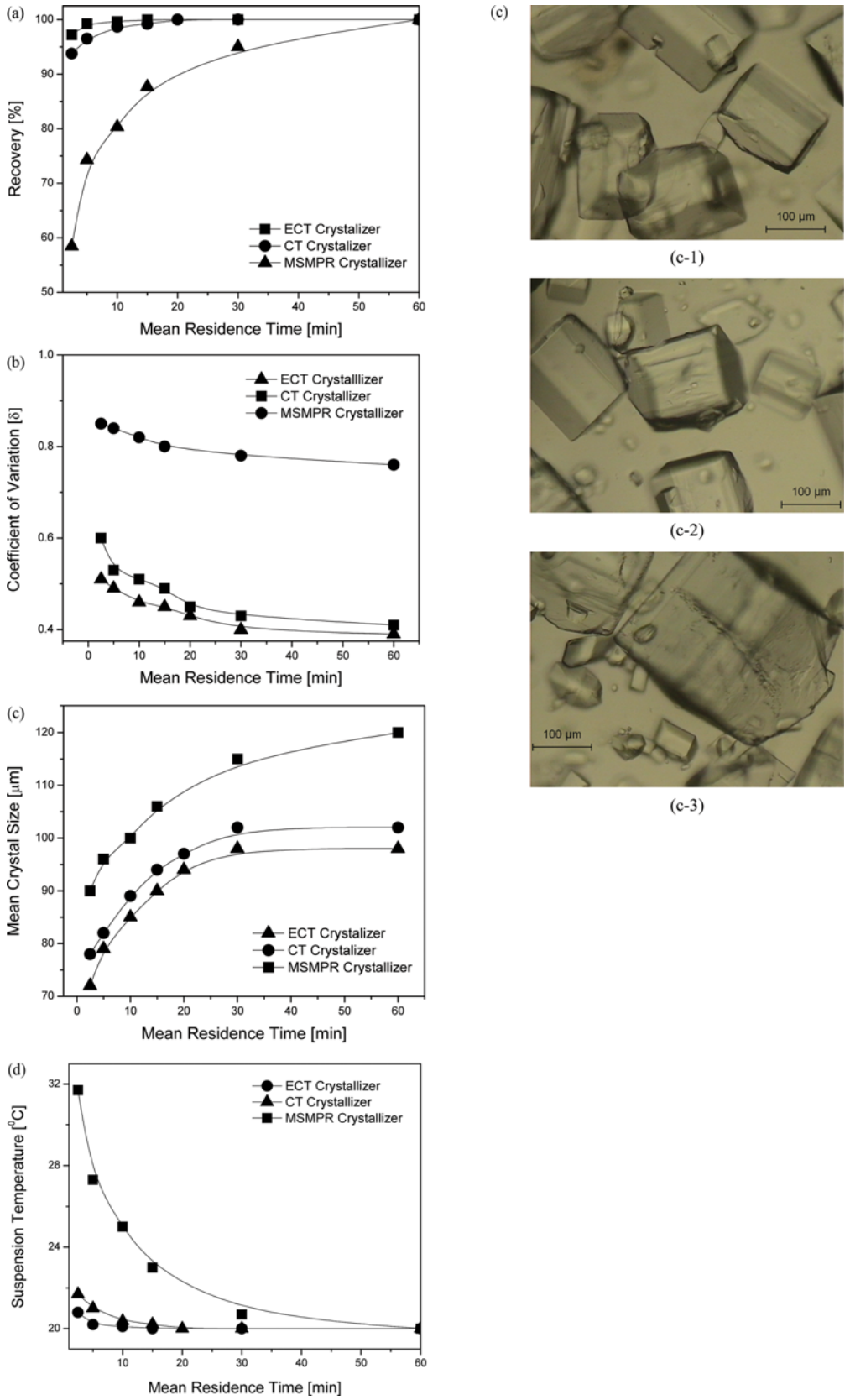

Fig. 7. Comparison of crystallization efficiency in terms of mean residence time in crystallizer when using feed solution temperature of 50 °C, cooling temperature of 20 °C, inner cylinder rotation speed of 700 rpm, and L-Lysine feed concentration of 900 g/l: (a) recovery, (b) crystal size and size distribution, (c) typical shape of crystal: (c-1) for ECT and (c-2) for CT crystallizer, and (c-3) for MSMPR crystallizer, (d) suspension temperature.

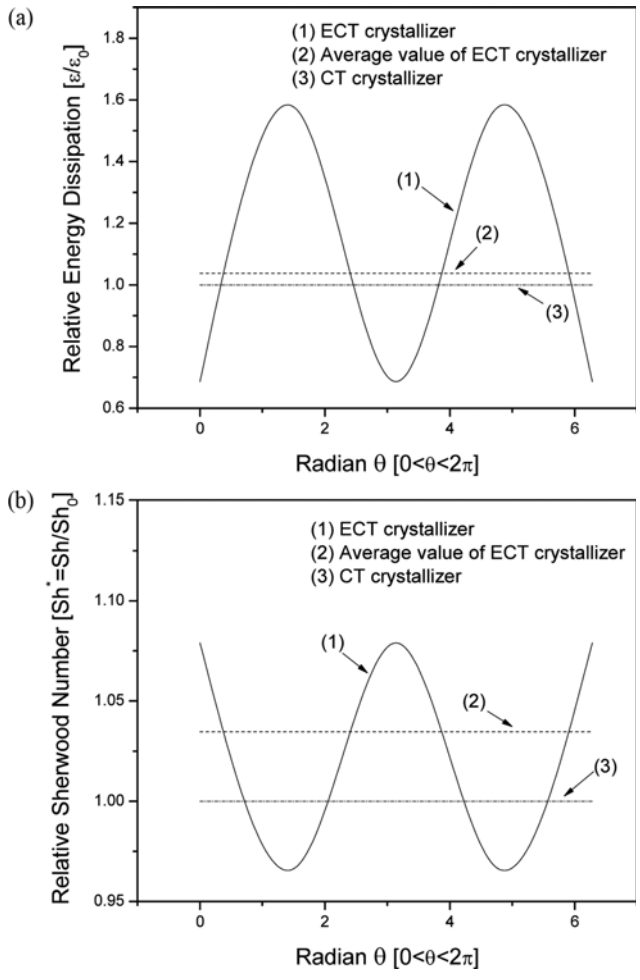

Fig. 8. Comparison of typical profiles of Taylor vortex flow in ECT and CT crystallizers in terms of (a) relative energy dissipation and (b) relative Sherwood numbers.

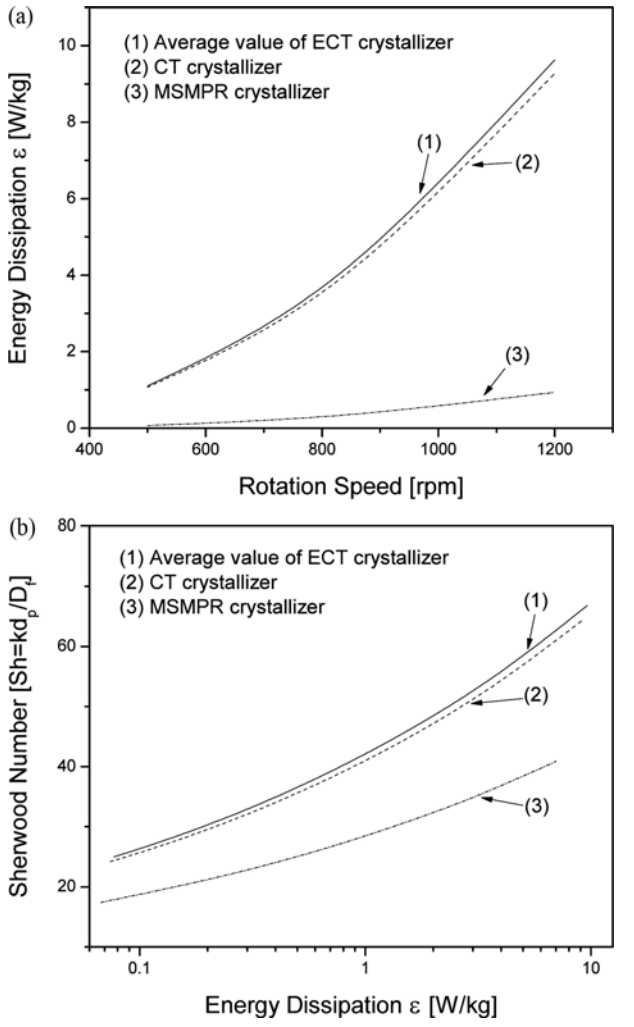

Fig. 9. Comparison of crystallization efficiency in ECT, CT, and MT crystallizers in terms of (a) energy dissipation and (b) relative Sherwood numbers.

that the peak viscous energy dissipation of the sinusoidal fluid motion was 60% higher than that of the circular azimuthal fluid motion, although its average value for the sinusoidal fluid motion was close to that for the circular motion. A similar result between the two flow motions was also observed for the mass transfer profiles.

According to Hirasawa et al. [19], external energy input promotes crystal nucleation by overcoming the energy barrier for nuclei. Thus, the high peak sinusoidal profile of viscous energy dissipation was more effective in promoting crystal nucleation than the flat profile of the circular fluid motion. This may explain the higher crystallization efficiency of the ECT crystallizer over that of the CT crystallizer.

As shown in Fig. 9, the viscous energy dissipation and mass transfer of the fluid motions in the crystallizers were estimated according to the rotation speed. For the whole range of rotation speeds, the viscous energy dissipation and mass transfer were much higher in the sinusoidal and circular Taylor vortices than in the random turbulent eddy. The difference in the viscous energy dissipation between the Taylor vortices and the random turbulent eddy was also amplified when increasing the rotation speed. The high efficiency of a Taylor vortex for energy dissipation can be explained in terms of the large contact surface of the inner cylinder with the solution, allowing an effective viscous transfer of momentum to the fluid. Thus, the high velocity profiles of the vortex motions produced a high viscous energy dissipation in the fluid.

CONCLUSIONS

The present study demonstrated that a sinusoidal Taylor vortex flow in an ECT crystallizer was effective for the cooling crystallization of L-lysine. Due to the high turbulent intensity of the sinusoidal Taylor vortex, crystal nucleation and growth were both significantly facilitated, which resulted in a 100% crystal recovery of L-lysine in the continuous ECT crystallizer within a mean residence time of 15 min when using moderate operation conditions of 700 rpm for the inner cylinder and 900 g/*l* for the feed concentration. The crystal size distribution was also significantly enhanced. These results indicate that the crystallization efficiency of the ECT crystallizer was four-times higher than that of the MSMPR crystal-

lizer. Furthermore, based on the sinusoidal intensity profiles, the sinusoidal Taylor vortex was found to be even more effective for the crystallization than the circular Taylor vortex.

ACKNOWLEDGEMENT

This work was supported by the Engineering Research Center of the Excellence Program of the Korean Ministry of Science, ICT & Future Planning (MSIP)/National Research Foundation of Korea (NRF) (Grant NRF-2014R1A5A1009799)

SUPPORTING INFORMATION

Additional information as noted in the text. This information is available via the Internet at http://www.springer.com/chemistry/journal/11814.

REFERENCES

1. R. Davey and J. Garside, *From Molecules to Crystallizers*, Oxford University Press (2000).
2. N. Anh-Tuan, J. M. Kim, S. M. Chang and W. S. Kim, *Ind. Eng. Chem. Res.*, **49**, 4865 (2010).
3. K. Kataoka, N. Ohmura, M. Kouzu, Y. Simamura and M. Okubo, *Chem. Eng. Sci.*, **50**, 1409 (1995).
4. E. Dluska, J. Wolinski and S. Wronski, *Chem. Eng. Technol.*, **28**, 1016 (2005).
5. J. G. Sczechowski, C. A. Koval and R. D. Noble, *Chem. Eng. Sci.*, **50**, 3136 (1995).
6. U. B. Holeschovsky and C. L. Cooney, *AIChE J.*, **37**, 1219 (1991).
7. R. L. C. Giordano, R. C. Giordano and C. L. Cooney, *Process Biochemistry*, **35**, 1093 (2000).
8. S. H. Kang, S. G. Lee, W. M. Jung, M. C. Kim, W. S. Kim, C. K. Choi and R. S. Feigelson, *J. Cryst. Growth*, **254**, 196 (2003).
9. W. M. Jung, S. H. Kang, W. S. Kim and C. K. Choi, *Chem. Eng. Sci.*, **55**, 733 (2000).
10. O. Richer, H. Hoffman and B. Kraushaar-Czarnetzki, *Chem. Eng. Sci.*, **63**, 3504 (2008).
11. M. N. Noui-Mehidi, A. Salem and P. Legentilhomme, *J. Legrand, Int. J. Heat and Fluid Flow.*, **20**, 405 (1999).
12. A.-T. Nguyen, T. Yu and W.-S. Kim, *J. Crys. Grow.* (2017), DOI: 10.1016/j.jcrysgro.2016.10.020.
13. V. Sinevic, R. Kuboi and A. W. Nienow, *Chem. Eng. Sci.*, **41**, 2915 (1986).
14. K. Atsumi, T. Makino and K. Kato, *Kagaku Kogaku Ronbunshu.*, **14**, 16 (1988).
15. S. Nakahara, *Kagaku Kogaku Ronbunshu.*, **3**, 435 (1977).
16. W. L. McCabe, J. C. Smith and P. Harriott, *Unit Operations of Chemical Engineering 6th*, McGraw Hill, Boston (2001).
17. K. Kikuchi, Y. Tadakuma, T. Sugawara and H. Ohashi, *J. Chem. Eng. Japan*, **20**, 134 (1987).
18. N. Anh-Tuan, Y. L. Joo and W. S. Kim, *Cryt. Growth Des.*, **12**, 2780 (2012).
19. M. Kurotani and I. Hirasawa, *J. Cryst. Growth*, **310**, 4576 (2008).

Supporting Information

Effect of sinusoidal Taylor vortex flow on cooling crystallization of L-lysine

Anh-Tuan Nguyen and Woo-Sik Kim†

Department of Chemical Engineering, Functional Crystallization Center, Kyung Hee University,
Seocheon-dong, Giheung-gu, Yongin-si 17104, Korea
(*Received 25 November 2016 • accepted 3 March 2017*)

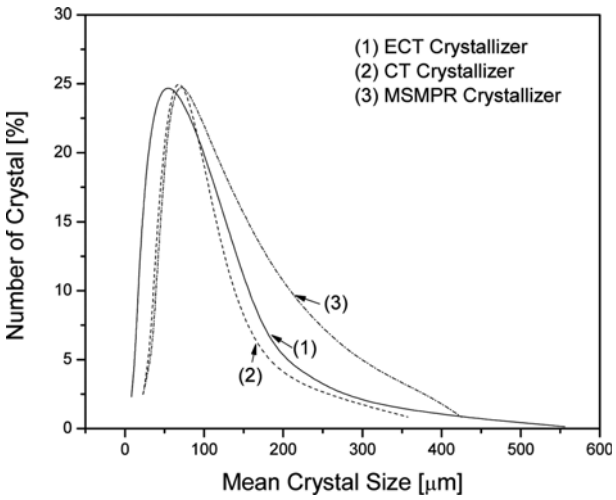

Fig. S1. Typical crystal size distribution of L-Lysine crystals in ECT, CT, and MSMPR crystallizers with various mean residence times when using feed solution temperature of 50 °C, cooling temperature of 20 °C, inner cylinder rotation speed of 700 rpm, and L-Lysine feed concentration of 900 g/*l*.